SolarPACES 2024, 30th International Conference on Concentrating Solar Power, Thermal, and Chemical Energy Systems

Thermal Energy Storage Materials, Media, and Systems

https://doi.org/10.52825/solarpaces.v3i.2512

© Authors. This work is licensed under a Creative Commons Attribution 4.0 International License

Published: 09 Oct. 2025

Design Features and Material Selection Methodology of High-Temperature Particle-Based Thermal Energy Storage Bin

Nader S. Saleh^{1,2,*}, Shaker Alaqel³, Rageh Saeed^{1,2}, Eldwin Djajadiwinata^{1,2}, Hany Al-Ansary^{1,2}, Abdelrahman El-Leathy^{1,2,4}, Syed Danish⁵, Zeyad Al-Suhaibani¹, and Sheldon Jeter⁶

¹Mechanical Engineering Department, King Saud University, Saudi Arabia
²K.A.CARE Energy Research and Innovation Center at Riyadh, Saudi Arabia
³Sandia National Laboratories, Mechanical Engineering, PhD, USA
⁴Mechanical Power Engineering Dept., Helwan University, Egypt
⁵Sustainable Energy Technologies Center, King Saud University, Saudi Arabia
⁶Georgia Institute of Technology, School of Mechanical Engineering, USA
*Correspondence: Nader S. Saleh, nader.alhabtary@outlook.com

Abstract. This study investigates the thermal performance of a novel particle-based thermal energy storage (TES) system. A small-scale TES bin was constructed using masonry materials in a multi-layered configuration. The primary objectives were to measure heat loss through the bin's wall and assess the thermal conductivity of the calcium silicate (Ca-Si) material, the insulating layer, at elevated temperatures. Heat transfer rates were determined using two independent methods, with results showing a minimal discrepancy of 3%. The thermal conductivity of the Ca-Si was found to be 0.115 W/m·K, indicating its effectiveness as a thermal insulator. Additionally, the expansion joint (EJ) layer successfully recovered its original thickness after cooling, demonstrating its ability to mitigate stresses resulting from the thermal expansion of inner layers. These findings support the scalability and efficiency of the proposed particle-based TES system design.

Keywords: Particle-Based Thermal Energy Storage, Calcium Silicate, Concentrated Solar Power

1. Introduction

Thermal energy storage (TES) technologies offer a promising solution for mitigating the intermittency of solar energy. TES systems enable the effective utilization of excess thermal energy generated during periods of high solar irradiation, allowing for its storage and subsequent use during periods of low or no solar input. The TES system is one of the key components in concentrated solar power (CSP) plants; it plays a crucial role in enhancing operational flexibility and improved dispatchability. Using solid particles as both a heat transfer and thermal energy storage medium overcomes temperature limitations of conventional media like molten salt or water, as they can withstand temperatures exceeding 1000 °C. The particle-based TES system comprises two main components: the particulate material and the containment structure. King Saud University (KSU) has conducted significant research related to both of these aspects. Several potential options for the particulate material have been investigated. These candidate

materials exhibit significant variations in terms of cost and performance [1]. For the containment structure, a simple and inexpensive design has been proposed and previously examined [2]. This design incorporates four layers, arranged from the innermost to the outermost as follows: (1) alumina-rich insulating firebrick, (2) perlite concrete with refractory cement, (3) expansion joint, and (4) reinforced concrete. However, this design faces two challenges: (1) the inherent brittleness of the insulating firebrick, which erodes over time due to particle flow, reducing thermal performance and contaminating the particles [3], and (2) the shrinkage tendency of perlite aggregates. The insulating firebrick and perlite concrete layers serve as the thermal insulating layers of the TES system. To address these issues, calcium silicate was selected as a substitute for the insulating firebrick and perlite concrete layers due to its superior thermal and mechanical properties. An additional protective layer was introduced between the particles and the Ca-Si layer to mitigate erosion. This study aims to design, construct and test a small-scale particle-based TES system incorporating these materials.

2. Experimental setup and test procedure

A small-scale particle-based TES bin was built on a concrete platform, comprising a base, a wall, and a lid (Figure 1). The base was constructed from Ca-Si boards, each with dimensions of $0.3 \text{ m} \times 0.6 \text{ m} \times 0.05 \text{ m}$. These boards were cut and shaped to form a cylindrical structure with a diameter of 2.4 m. Fourteen levels of Ca-Si boards were stacked to achieve a base height of 0.7 m. The base was encased in a reinforced concrete (RC) shield to protect against environmental exposure and support the bin's wall and content.

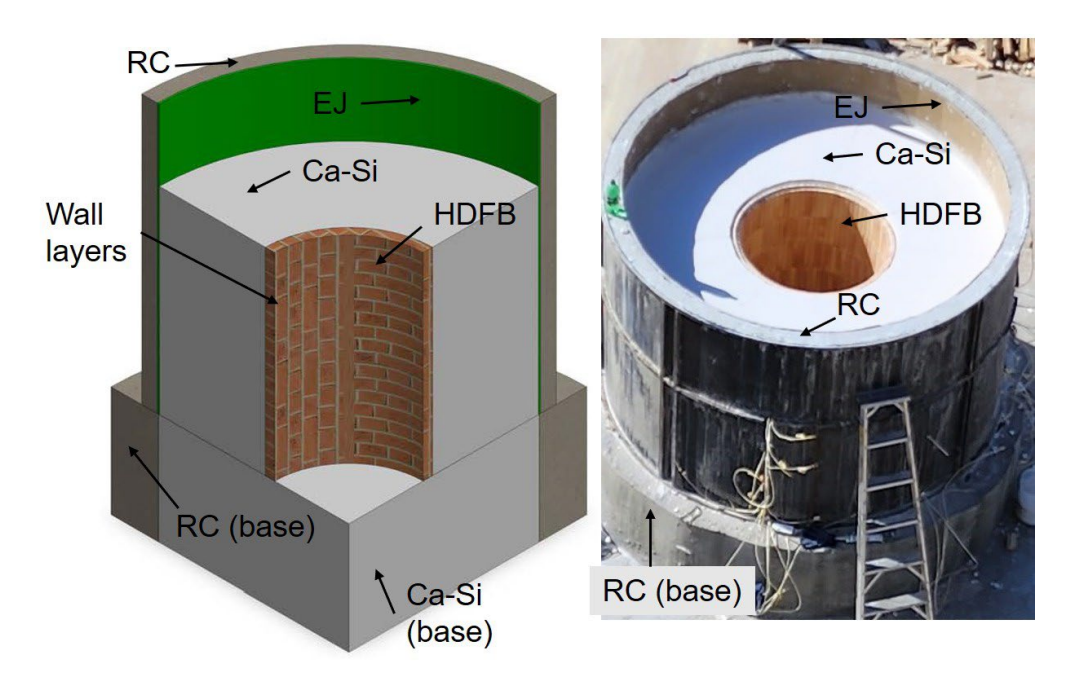


Figure 1. A 3D model and a photograph of the TES bin

The bin's wall, a multi-layered structure, was constructed on top of the base. It is composed of four layers arranged from innermost to outermost: (1) high-density firebrick (HDFB), (2) Ca-Si, (3) expansion joint (EJ), and (4) RC. The HDFB layer is made of Mullite firebricks that include 75% alumina. To ensure the integrity of this layer, the Mullite firebricks were specifically designed and manufactured to have an interlocking feature as illustrated in Figure 2a. With this feature, the bin's inward collapse is avoided, no mortar is required, and the assembly becomes easier. These bricks demonstrated excellent thermal shock resistance, enduring 25 cycles of heating to 1000 °C and quenching in water without cracking or spalling. The HDFB layer primarily protects the Ca-Si layer from particle-induced erosion. The Ca-Si layer was constructed from calcium silicate boards, Figure 2b. The Ca-Si offers several advantages, in-

cluding lower thermal conductivity, greater mechanical stability, lower cost, and most importantly, it can operate at temperatures up to 1100 °C. The EJ layer serves as a damper, absorbing thermal stresses from the HDFB and Ca-Si layers. It is made of recycled bitumen fiber, Figure 2c. It has high compression and recovery rates (95%) and a compressive strength ≥ 2 MPa. The outermost layer was constructed from RC to provide structural integrity and environmental protection. The wall construction was performed as follows: (1) building the RC shell (outermost layer), (2) installation of the expansion joint layer on the RC shell, and (3) simultaneous assembly of the HDFB and Ca-Si layers.

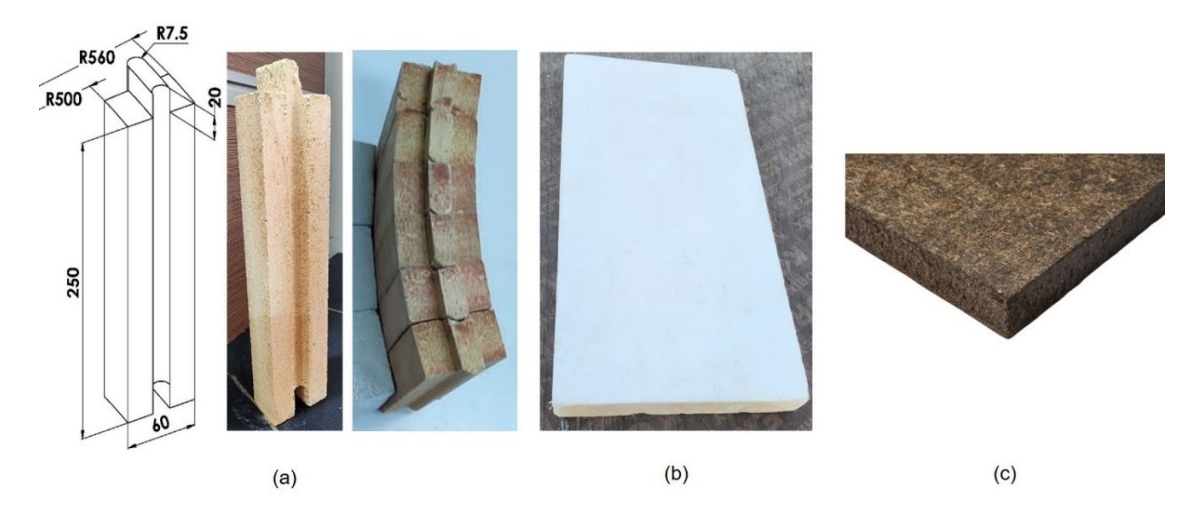


Figure 2. (a) Mullite bricks, dimensions in mm, (b) Ca-Si board, and (c) recycled bitumen fiber board

The HDFB layer comprises five vertically stacked levels of interlocking bricks (each 0.25 m high and 0.06 m thick), resulting in a bin height of 1.25 m. Construction of the HDFB and Ca-Si layers started by assembling the first level of interlocking bricks, followed by the installation of five corresponding levels of Ca-Si boards circumferentially enveloping the HDFB layer. This iterative process was repeated until the completion of five HDFB levels and 25 Ca-Si levels. Figure 3 illustrates the progressive construction of these two layers until fully completed. The interlocking bricks were engineered to form a cylindrical structure with an approximate inner diameter of 1 m. Concurrently, the CaSi rectangular boards were cut and shaped on-site to conform to a cylindrical configuration, achieving a uniform thickness of approximately 0.668 m.



Figure 3. Construction progress of the HDFB and Ca-Si layers

Upon completion of the wall construction, the bin became ready for experimental evaluation. This test aims to analyze the wall's effectiveness in minimizing heat loss. The experiment utilized heated, stagnant particles as the storage medium. The bin was filled with approximately 1.3 metric tons of white sand, with an average diameter of 0.3 mm and a bulk density of 1550 kg/m³. Electric resistance heaters served as the thermal energy source, comprising four heating coils, each with a power rating of approximately 6.5 kW and made from Kanthal-A1 wire. These coils were strategically positioned within the bin at vertical intervals of 0.25 m. The filling of the bin and the installation of the heating coils were performed concurrently, with sand poured to predetermined heights, followed by the placement of each coil, as depicted in Figure 4. Heater operation was regulated by a sophisticated control panel equipped with four proportional-integral-derivative (PID) controllers, contactors, and switches. Surface temperatures of the heating coils were monitored using Type-K thermocouples, each encased in a 0.1 m-long ceramic tube positioned within the coil, with the resulting data relayed to the PID controller for precise thermal regulation. Each heater operated independently to ensure uniform heating. Following the completion of the sand filling process, the bin was sealed with a lid. The lid was constructed from Ca-Si boards, eight levels of shaped Ca-Si boards were stacked to form a lid with a height of 0.4 m, arranged to cover the bin's inner diameter.

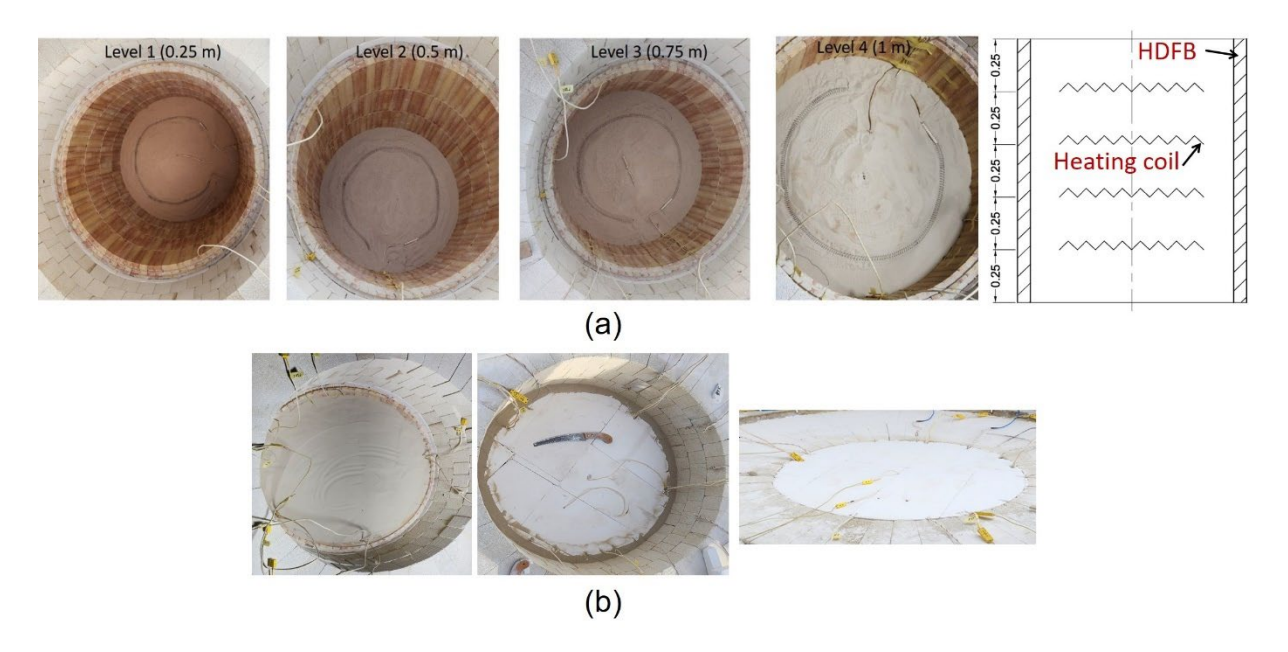


Figure 4. (a) Filling the bin and installing the heaters, (b) lid installation

To evaluate the performance of the TES bin, critical parameters including temperatures, heat flux, and the thickness of the EJ layer were measured. Therefore, an array of calibrated Type-K thermocouples (XC-K, Omega Engineering Inc.) and thin-film heat flux sensors (HFS-3, Omega Engineering Inc.) were deployed at designated locations within the bin's multi-layered wall structure. The thermocouples, pre-calibrated to ensure measurement accuracy, were installed to capture the temperature variations across the wall's layers. Specifically, thermocouples were arranged at three distinct vertical levels, as illustrated in Figure 5, to monitor interface temperatures between adjacent layers: one thermocouple (TC) positioned at the inner surface of the HDFB layer, another at the HDFB-Ca-Si interface, a third at the Ca-Si-EJ interface, and a fourth at the EJ-RC interface. The installation methodology, also depicted in Figure 5, was designed to optimize measurement precision. To enhance contact between the thermocouples and the wall, grooves were created on both sides of the Ca-Si board, enabling direct contact with the HDFB and Ca-Si layers on one side and the Ca-Si and EJ layers on the opposite side. The average thickness of the Ca-Si layer is approximately 0.668 meters.



Figure 5. Thermocouples distribution, dimensions are in meter, (left) side view, (right) top view

To quantify the heat loss through the multi-layered wall, two thin-film heat flux sensors were attached to the inner surface of the EJ layer, specifically positioned at the mid-height of the bin, positioned 90 degrees apart in the radial direction to capture representative heat flux measurements across the cylindrical structure. These sensors were securely adhered using a silicone-based adhesive, ensuring optimal contact and sustained measurement integrity. Figure 6a illustrates the detailed placement and configuration of the installed sensors. All thermocouples and heat flux sensors were wired to a data acquisition unit (Keysight 34972A) to acquire their signals for analysis of the bin's thermal performance.

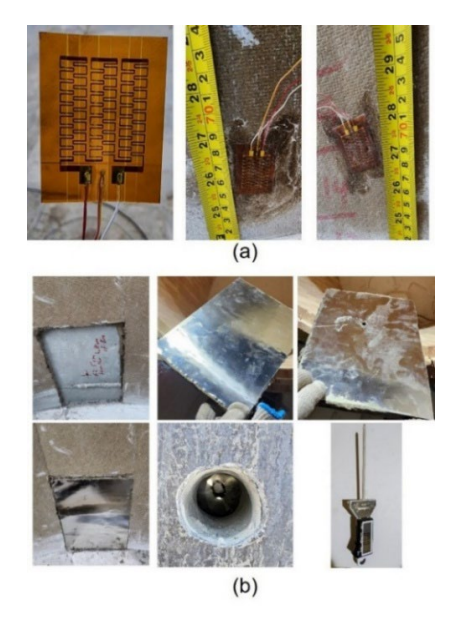


Figure 6. (a) The heat flux sensors, (b) Implemented methodology to quantify the layers expansion

To quantify the thermal expansion of the wall's layers (HDFB and Ca-Si) due to elevated temperatures, the following methodology was implemented. A rectangular segment measuring 0.2 m by 0.3 m was extracted from the EJ layer at the mid-height of the bin. A through-hole was then created within this segment. Two stainless-steel foils were applied to cover both surfaces of the EJ segment; one foil, featuring a perforation aligned with the through-hole in the EJ segment, was oriented toward the RC layer, while the unperforated foil faced the Ca-Si layer. Subsequently, a larger concentric hole was drilled in the RC layer, ensuring alignment with the EJ segment's through-hole. By measuring the thickness of this segment, the thermal expansion of the HDFB and Ca-Si layers can be quantified. A depth gauge was used to measure the thickness as temperature varied. The mid-height location was selected since it is farthest from end effects, such as thermal gradients or structural constraints near the base or lid, thereby providing a representative measurement of the fundamental material response of the EJ layer. Figure 6b illustrates the sequential stages of this measurement tool preparation.

3. Results

Following the complete filling of the bin with white sand and the secure installation of the Ca-Si lid, the heaters were activated. The heating process was sustained until the sand attained a steady-state thermal condition. As depicted in Figure 7, the temperature at the bin's center stabilized at approximately 700 °C, a level consistently maintained over several days, demonstrating the system's capacity to achieve and sustain high-temperature operation.

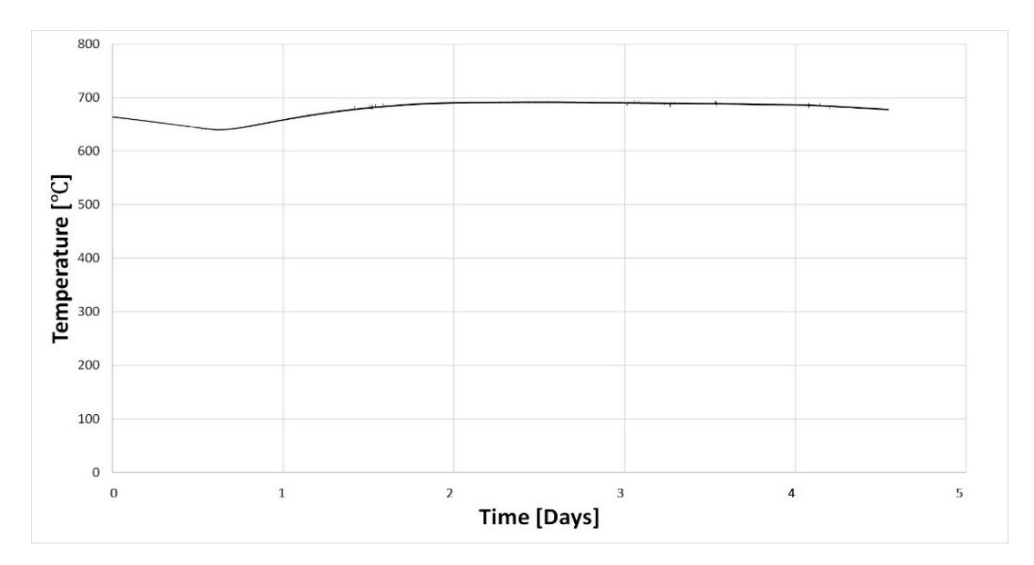


Figure 7. White sand temperature at the bin's center

Figure 8 illustrates the temperatures of the wall layers, specifically the inner and outer surface temperatures of the HDFB, Ca-Si, and EJ. The data confirm the attainment of a steady-state thermal condition, indicating stable operation of the system. Qualitatively, the Ca-Si layer demonstrates exceptional performance as a thermal insulator, effectively suppressing heat flow through the bin's wall and thereby minimizing heat losses.

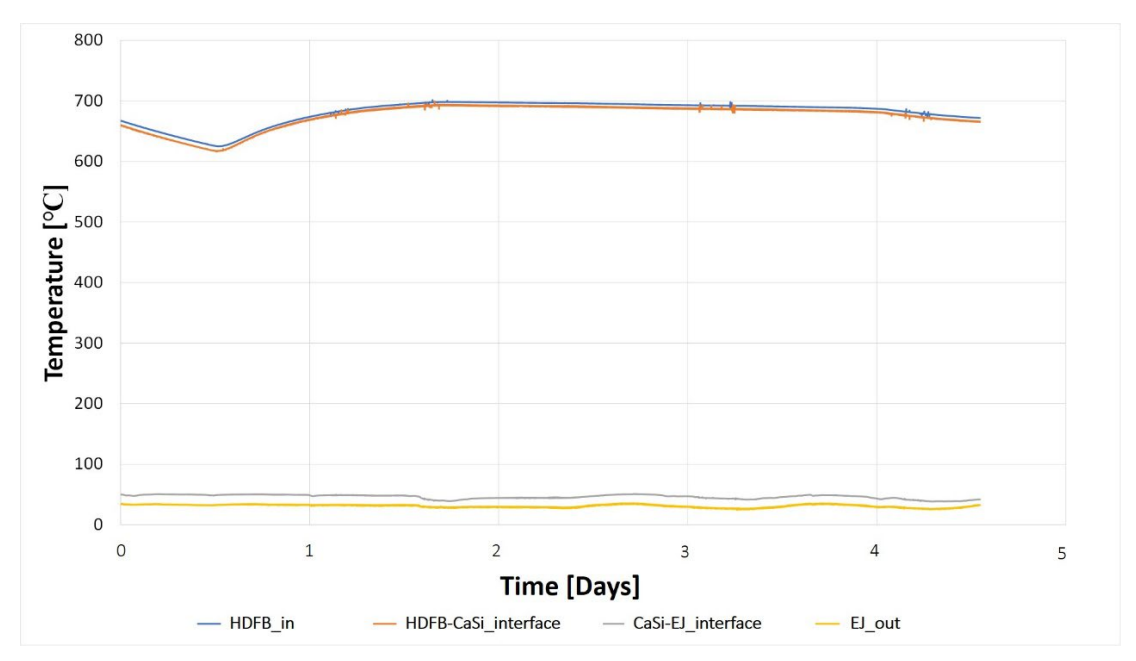


Figure 8. Temperatures of the wall layers

Temperature measurements recorded on the third day (Day 3) of steady-state operation were averaged to facilitate detailed analysis. The resulting mean values are presented in Table

1, providing an overview of the thermal performance across the bin's multi-layered wall structure.

Table 1. Average temperatures of the wall's layers

Location	HDFB inner surface	HDFB-CaSi interface	CaSi-EJ interface	EJ outer surface
Temperature [°C]	695.4	690.1	46.9	31.0

The heat loss through the bin's wall was quantified using two methods. The first method employed direct measurements of heat flux at the inner surface of the EJ layer (Figure 6a). The second method utilized thermal properties of the EJ layer, specifically the temperature difference across the layer and its thermal resistance. For the first method, the heat flux was continuously monitored throughout the experiment, yielding an average heat flux of 75.6 W/m² on Day 3. Consequently, the heat transfer rate was calculated using the following equations:

$$\dot{Q}_w = q_m^{\prime\prime} A_{ELi} \tag{1}$$

$$A_{EI,i} = \pi D_{EI,i}L \tag{2}$$

where q_m'' is the measured heat flux, $A_{EJ,i}$, $D_{EJ,i}$ are the inner surface area and inner diameter of the EJ layer, respectively, and L is the height of the bin.

The original inner diameter of the EJ layer, measured prior to the initiation of the experiment, was 2.389 m. As the heating process began, the rising temperature of the sand induced a corresponding increase in the temperatures of the inner layers (HDFB and Ca-Si). Consequently, these layers expanded against the EJ layer, resulting in its compression and a subsequent increase in both its inner diameter and inner surface area. A key objective of this experiment was to evaluate the ability of the EJ layer material to relieve thermal stresses imposed on the inner layers due to temperature increase and to verify its capability to recover its original thickness upon cooling of the bin. To validate this hypothesis, the thickness of the EJ layer was measured using the methodology described previously (Figure 6b), with measurements taken both before the experiment and when the sand temperature approached 700 °C. Results indicated minimal compression of the EJ layer (10%) due to the expansion of the two inner layers, corresponding to a thickness reduction of 1.22 mm. As the expansion was directed outward, the EJ layer's inner diameter increased while its outer diameter remained constant due to confinement against the RC layer. Utilizing the updated inner diameter and corresponding surface area, the measured heat transfer rate was determined to be 710 W. The second method for determining the heat transfer rate through the wall involved calculations based on the EJ layer's thermal properties. By employing the known thermal conductivity and the updated thickness (or diameter) of the EJ layer, the thermal resistance R_{EI} of the EJ layer can be calculated and the heat transfer rate is then determined as follows

$$R_{EJ} = \frac{\ln\left[\frac{D_{EJ,o}}{D_{EJ,i}}\right]}{2\pi L k_{EJ}} \tag{3}$$

$$\dot{Q}_{w} = \frac{\Delta T_{EJ}}{R_{EJ}} \tag{4}$$

where $D_{EJ,o}$ is the outer diameter, k_{EJ} is the thermal conductivity and ΔT_{EJ} is the temperature difference across the EJ layer.

The thermal conductivity of the EJ material was measured in the laboratory using the HFM 436 Lambda device (Netzsch). By employing the average value of the inner and outer surface temperatures across the EJ layer, the thermal conductivity was determined to be 0.049 W/m·K. Substituting this value into Equation 3 and then using Equation 4, the heat transfer rate through

the wall (\dot{Q}_w) was calculated to be 687.2 W. The corresponding heat flux at the inner surface of the EJ layer was computed as 73.18 W/m². A comparison between the measured and calculated heat transfer rates revealed a marginal discrepancy of 3%, which is well within the 10% error band stated by the manufacturer of the HFS, affirming the reliability of the methodologies. This excellent agreement is expected since both the EJ layer and the HFS are near the outside of the bin away from elevated temperatures. Furthermore, the bin was shaded from solar radiation heating which is known to influence these measurements. In addition to the primary objective of quantifying heat loss through the bin's wall, a secondary aim was to evaluate the thermal conductivity of the Ca-Si layer at elevated temperatures. Given that the heat transfer rate across the wall layers remains constant under steady-state conditions, the thermal conductivity (k_{Ca-Si}) of the Ca-Si material can be determined as follows:

$$k_{Ca-Si} = \frac{\dot{Q}_w \ln[D_{Ca-Si,o}/D_{Ca-Si,i}]}{2\pi L \Delta T_{Ca-Si}}$$
 (5)

By substituting the relevant parameters into Equation 5, the thermal conductivity (k_{Ca-Si}) of the Ca-Si material was determined to be 0.115 W/m·K, confirming its efficacy as a thermal insulator at elevated temperatures. Upon conclusion of the experiment, the bin was allowed to cool to ambient conditions. Subsequent measurement of the EJ layer's thickness revealed that it had fully recovered to its original value, demonstrating its robust capacity to accommodate and mitigate thermal expansion stresses without permanent deformation.

4. Conclusions

A small-scale particle-based TES bin was designed, constructed and tested at a high temperature of 700 °C using electric heaters to elevate the temperature of white sand. The experiment successfully quantified heat loss through the bin's multi-layered wall, with measured and calculated heat transfer rates exhibiting a minimal discrepancy of 3%, thereby validating the accuracy and reliability of the employed methodologies. The thermal conductivity of the Ca-Si material was determined to be 0.115 W/m·K, indicating its suitability as a thermal insulator at elevated temperature conditions. This characteristic is essential for optimizing the efficiency of thermal energy storage systems. Furthermore, the EJ layer demonstrated the ability to recover to its original thickness after cooling, highlighting its effectiveness in alleviating stresses induced by the thermal expansion of the inner layers during operation. This characteristic is crucial for the long-term durability of the TES system. Collectively, these findings are promising for the scalability of the particle-based TES system using the design outlined in this study.

Data availability statement

The experimental datasets generated during the current study are available from the corresponding author on reasonable request.

Author contributions

Conceptualization, N.S.S., S.A., S.J., H.A.-A., E.D.; Methodology, N.S.S., S.A., E.D., S.J.; Resources, H.A.-A.; Investigation, N.S.S., S.A., E.D., R.S.; Formal analysis, N.S.S., S.A.; Visualization, N.S.S.; Validation, H.A.-A., R.S., A.E.-L., Z.A.-S., S.N.D.; Data Curation, Z.A.-S., S.N.D.; Writing - Original Draft, N.S.S.; Writing - Review & Editing, N.S.S., E.D., S.J.; Supervision, H.A.-A., A.E.-L., Z.A.-S.; Funding acquisition, H.A.-A.; Project administration, H.A.-A., S.A., N.S.S.

Competing interests

The authors declare that they have no competing interests.

Acknowledgement

The authors would like to express their profound gratitude to King Abdullah City for Atomic and Renewable Energy (K.A.CARE) for their financial support in accomplishing this work.

References

- [1] Saeed, R. S., Alswaiyd, A., Saleh, N. S., Alaqel, S., Djajadiwinata, E., El-Leathy, A., ... & Almutairi, Z. (2022). Characterization of low-cost particulates used as energy storage and heat-transfer medium in concentrated solar power systems. Materials, 15(8), 2946. Doi: https://doi.org/10.3390/ma15082946.
- [2] El-Leathy, A., Jeter, S., Al-Ansary, H., Danish, S. N., Saeed, R., Abdel-Khalik, S., ... & Al-Suhaibani, Z. (2019). Thermal performance evaluation of lining materials used in thermal energy storage for a falling particle receiver based CSP system. Solar Energy, 178, 268-277. Doi: https://doi.org/10.1016/j.solener.2018.12.047.
- [3] Al-Suhaibani, Z., Saleh, N. S., Alaqel, S., Saeed, R., Djajadiwinata, E., Danish, S. N., ... & Jeter, S. (2024). Vulnerability of Thermal Energy Storage Lining Material to Erosion Induced by Particulate Flow in Concentrated Solar Power Tower Systems. Materials, 17(7), 1480. Doi: https://doi.org/10.3390/ma17071480.